

## TIME DOMAIN SIMULATIONS OF BEAM-LOADING

S.KOSCIELNIAK

TRIUMF, 4004 Wesbrook Mall, Vancouver B.C., V6T 2A3 Canada.

Abstract. We present the results of computer simulations of high current beam loading in a proton storage ring. The model integrates the differential equation for gap voltage, and iterates the difference equations for particle longitudinal motion. The effects of cavity fields on the bunch shape and of the fundamental component of the beam on the cavity are treated in a self-consistent manner. The simulation model is applied to verify the dipole-quadrupole hybrid Robinson instability criterion, which differs from the dipole-mode criterion.

### INTRODUCTION

An analysis of particle beam stability proceeds by finding the electromagnetic fields induced in the environment by the passage of the beam, and then the reaction upon the beam of these fields. Often the environment is represented by its impedance, and its effect by a potential difference. The frequency domain relation between current  $I$  and voltage  $V$  is :

$$V(\omega) = Z(\omega) \times I(\omega) . \quad (1)$$

Here  $\omega$  is the angular frequency and  $Z$  is the complex impedance. When quantities are sinusoidal wave-trains of infinite duration, the same multiplicative relation holds in the time domain. However, this corresponds to a beam that never changes. For the simulation of a particle beam instability the instantaneous harmonic components are expected to change amplitude and/or phase at each time-step. In this case, use of relation (1) is inconsistent with the model and over-looks the transient response of the impedance. Instead, the time domain simulation must use the convolution integral

$$V(t) = \int_{-\infty}^t Z(t-t')I(t')dt' \quad (2)$$

or an equivalent formulation. For the particular case of beam-loading, a less cumbersome approach can be used.

### BEAM LOADING MODEL

Robinson instability<sup>1</sup> may arise when a charged particle beam interacts with a narrow band resonant impedance. Beam-loading refers to the case where the bunched beam fundamental harmonic component excites the accelerating cavities. The response of the cavity is modelled by a parallel resonant circuit ; with lumped capacitance  $C$ , inductance  $L$  and

resistance  $R$ . Let  $k = 1/(RC)$  be the decay time constant, and  $\omega_0 = 1/\sqrt{LC}$  the resonant frequency. The differential equation governing accelerating voltage is :

$$\ddot{V} + 2k\dot{V} + \omega_0^2(t)V = 2kR\dot{I}_T(t). \quad (3)$$

The dot notation indicates a time derivative.  $I_T$  is the sum of the generator current sinusoid and the (instantaneous) fundamental component of the beam image current, a function which looks like :

$$I_T(t) = I_g e^{j\phi_g} e^{\pm j\omega t} + I_b(t) e^{j\phi_b(t)} e^{\pm j\omega t}. \quad (4)$$

In the absence of control loops the generator amplitude  $I_g$  and phase  $\phi_g$  are constants. However, the beam function reproduces FM side-bands at multiples of the synchrotron frequency ( $\Omega_s$ ) if the phase varies as  $\phi_b(t) = \phi_0 \cos(\Omega_s t)$ , and AM side-bands if the amplitude varies as  $I_b(t) = I_b^0 \cos(4\Omega_s t)$ . Consequently, the model incorporates both the dipole and quadrupole bunch oscillation modes, etc.. In the simulation, the terms  $\phi_b(t)$  and  $I_b(t)$  are found by Fourier analysing the bunch shape at each integration step. Between the steps, the quantities are assumed to change linearly, thereby avoiding infinities in the derivative of  $I_T$ . Since the drive-term in equation (3) is piece-wise linear, the cavity voltage can be found exactly by the method of complementary function<sup>2</sup>. The general solution is :

$$V(t) = (M \times t + m) e^{j\mu} e^{\pm j\omega t} + N \times \exp(-kt) e^{j\nu} e^{\pm j\omega' t}. \quad (5)$$

The constants of integration ( $M, m, \mu, N, \nu$ ) are chosen from continuity conditions at each cavity crossing. The first term is the driven response and the second the transient response. The frequency of the transient components is  $\omega' = \sqrt{\omega_0^2 - k^2}$ , and the relation between the drive ( $\omega$ ) and resonance ( $\omega_0$ ) angular frequencies is obtained from the detuning condition :

$$\tan \psi \equiv (\omega_0^2 - \omega^2)/(\omega\omega_0/Q). \quad (6)$$

Here  $\psi$  is the tuning angle. Below transition energy,  $\omega_0 > \omega$  and  $\psi > 0$ .

## STABILITY INVESTIGATION

The analytic conditions (due to Robinson) for dipole-mode stability of a matched working point are : (i) to detune the cavity in the correct sense ( $\psi > 0$  below  $\gamma_t$ ), and (ii) provide rf-bucket area for coherent synchrotron oscillations ( $I_b/I_0 < \sin(2\psi)/2 \cos \phi_b$ ). However, it is unclear from the conditions what the precise dynamical behaviour of the beam should be. For these reasons, investigation of the Robinson criteria is an ideal testing ground. Firstly, the code was tested by its ability to reproduce stable behaviour at the usual synchrotron working points, namely  $I_b/I_0 = \tan \psi$  and  $\phi_g = 0$ . Secondly, the focus of enquiry moved to alternative working points where there was still something new to be learnt.

## SIMULATIONS

The computer experiments were made with the particle tracking code LONG1D<sup>3,4</sup> which simulates the longitudinal phase-space motion of a proton synchrotron. The machine parameters were chosen to model the Triumf KAON Factory<sup>5</sup> Booster ring. The beam bunch

is modelled by a partially ordered ensemble of macro-particles. The small, finite number of simulation particles implies a statistical jitter in the bunch shape ; and hence, also in the phase and magnitude of the fundamental beam component. It is this feature of the model which is solely responsible for seeding any unstable behaviour that may occur.

A true observational test of stability requires the system to be watched indefinitely. Herein, we adopt a more practical definition of stability : no obvious growth of any dipole or quadrupole oscillation when the system is watched for  $\sim 30$  synchrotron oscillation periods.

### Matching

At the start of the simulation, the beam and rf-system have to be matched and in a state of equilibrium. The matching is achieved by adjusting the generator current amplitude and phase, as functions of  $I_b$ ,  $\phi_b$  and  $\psi$  according to the simultaneous relations :

$$I_0 = [I_g \cos \phi_g - I_b \sin \phi_b] \quad \text{and} \quad -I_0 \tan \psi = [I_g \sin \phi_g - I_b \cos \phi_b]. \quad (7)$$

Here  $I_0 = V_0/R$  where  $V_0$  is the nominal gap voltage. For a non-accelerating beam  $\phi_b = 0$ . Equilibrium is forced by setting the transient parts of the voltage solution (5) to zero as initial conditions. We shall call a  $(I_b/I_0, \psi)$  combination a working point.

## RESULTS

All of the working points<sup>6</sup> are summarised in a stability diagram, Figure 7 ; and a few demonstrative examples are presented as mountain range plots, Figures 1 through 6.

### Below the Robinson Limit

Figure 1 shows a stable beam with correct detuning :  $I_b/I_0 = 1$ . and  $\psi = (+)45^\circ$ . The bunch is elliptic in shape and has length  $50^\circ$ .

### Reverse detuning

Figure 2 shows the effect of detuning in the wrong sense :  $I_b/I_0 = 1$ . and  $\psi = (-)45^\circ$ . The beam is unstable, as expected from Robinson's first criterion.

### Above the Robinson Limit

Figure 3 shows the working point  $I_b/I_0 = 2.3$  and  $\psi = (+)45^\circ$ . Unexpectedly, the beam is stable. The transient motion, early on, occurs while the cavity-gap rf-phase moves (with an over-shoot) to match the (statistical) seed displacement of the bunch centre.

Figure 4 shows a working point slightly above that of figure 3 :  $I_b/I_0 = 2.41$  and  $\psi = 50^\circ$ . The beam is unstable, and breaks into violent dipole oscillations.

Figure 5 shows a similar working point to figure 3, namely  $I_b/I_0 = 3.0$  and  $\psi = 48^\circ$ . However, the bunch is much longer ( $120^\circ$ ), and in this case the beam is stable.

### Small Tuning Angles

The second Robinson criterion, implies that working points here should be stable. Figure 6 clearly demonstrates that this is not so. Notice how the instability starts as a gentle

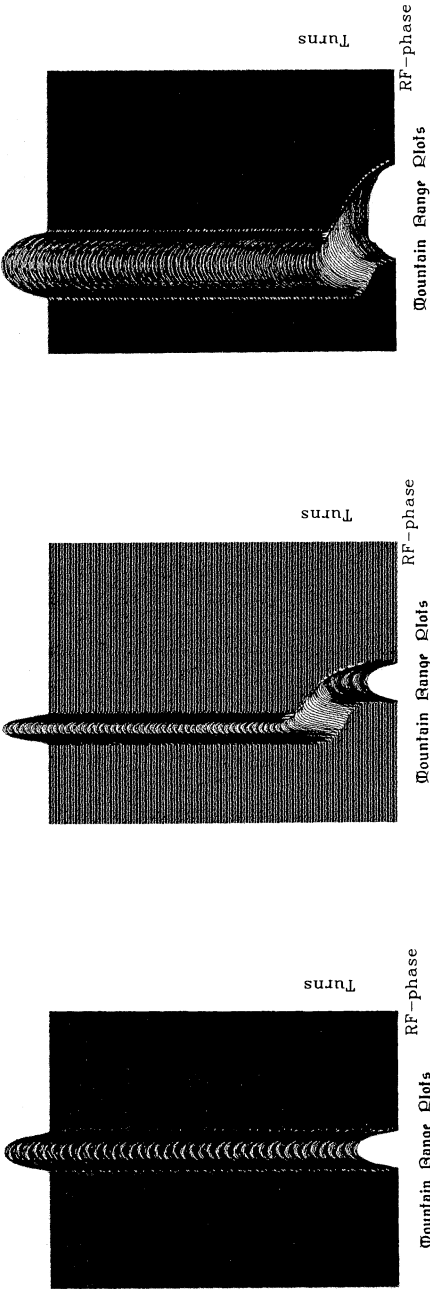


FIGURE 1

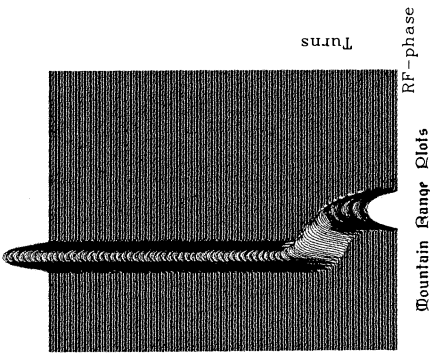


FIGURE 3

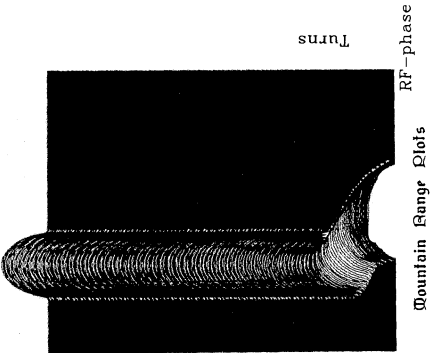


FIGURE 5

FIGURE 2

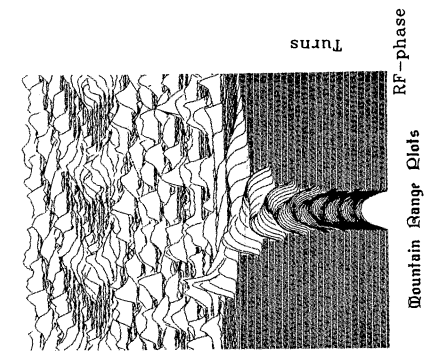


FIGURE 4

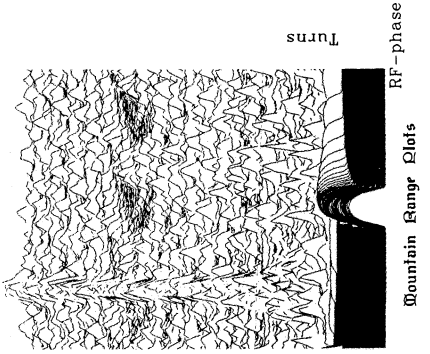


FIGURE 6

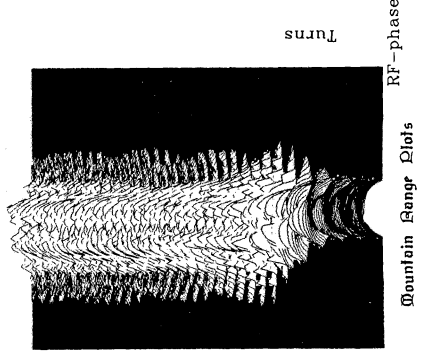
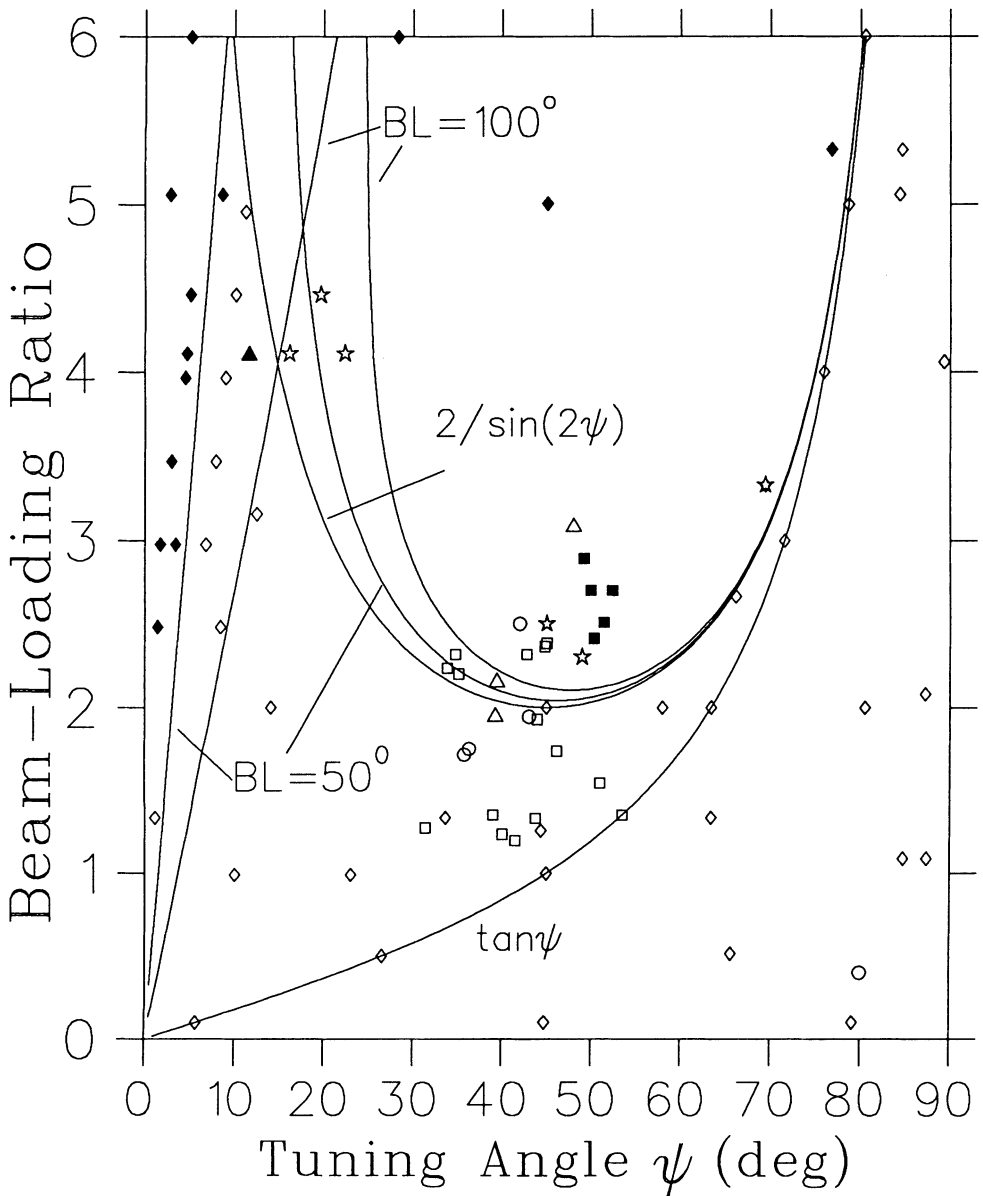


FIGURE 7 : Stability Diagram



- |                                    |   |                                  |   |
|------------------------------------|---|----------------------------------|---|
| $\square$ Stable, $BL=50^\circ$    | $\blacksquare$ Unstable, $BL=50^\circ$    | $\star$ Stable, $BL=100^\circ$   | $\circ$ Stable, $BL=199^\circ$          |
| $\triangle$ Stable, $BL=120^\circ$ | $\blacktriangle$ Unstable, $BL=120^\circ$ | $\diamond$ Stable, $BL=70^\circ$ | $\blacklozenge$ Unstable, $BL=70^\circ$ |

modulation of the bunch height and length and then transforms into an oscillation of the centroid ; evidently mode-coupling at work.

### EXPLANATION

Recent theoretical progress<sup>7,8</sup> shows that in the presence of dipole-quadrupole mode-coupling, the second Robinson condition should be replaced by :

$$1 + \left( \tan \psi - \frac{I_b}{I_0} \right) \left( \tan \psi - \frac{I_b \theta_0}{I_0} |f(\theta_0)| \right) > 0 \quad \text{and} \quad \frac{I_b}{I_0} < \frac{3 \tan \psi}{\theta_0 |f(\theta_0)|}. \quad (8)$$

The form factor<sup>7</sup>  $f(\theta)$  depends on the bunch length ( $2 \times \theta_0$ ) and shape, and so there is not one single stability curve but a range of curves for each bunch-shape. Together, conditions (8) give a stable working region which, for small tuning angles, is significantly different from the Robinson criteria. Qualitatively, short bunches are more stable than long ones for small tuning angles  $\psi < 30^\circ$  ; and long bunches are more stable than short ones for medium tuning angles  $\psi \sim 45^\circ$ .

In figure 7 we plot the bounding stability curves for bunch lengths (BL) of  $50^\circ$  and  $100^\circ$ , assuming elliptic bunch-shapes. The usual Robinson stability curve  $2/\sin(2\psi)$  is plotted for comparison. On the plot we have superimposed the results of the computer experiments : filled plotting symbols for unstable cases and open symbols for the stable working points. Different symbols are used to indicate the various bunch lengths used in the trials.

Note, in particular, the black diamonds indicating instability (for small tuning angle) below the Robinson limit ; and the open squares, stars etc. which indicate stability (for medium tuning angle) above the Robinson limit. In general, there is good agreement between the theoretical stability limits and the trials, but this is quantitatively not exact. Perhaps the discrepancy is due to coupling with other bunch-modes and/or the cavity response to higher synchrotron side-bands ; neither of which are included in the theoretical model.

### REFERENCES

1. F.J. Sacherer, Method for Computing Bunched Beam Instabilities, CERN/SI-BR/72-5.
2. J.H. Spencer, BEAM-LOAD, Beam Loading Supplement for LONG1D, TRI-DN-88-3.
3. S. Koscielniak, LONG1D, Users Guide, TRI-DN-88-20.
4. S. Koscielniak, The LONG1D Simulation Code, pg. 743, Proc. of European Particle Accelerator Conference, Rome 1988.
5. KAON Factory Proposal, TRIUMF Vancouver Canada, Sept. 1985.
6. S. Koscielniak, Computer Simulations of Beam Loading, TRI-DN-88-34.
7. S. Koscielniak, A General Theory of Beam Loading, TRI-DN-K25.
8. T.S. Wang, Bunched-Beam Longitudinal Mode-Coupling and Robinson-type Instabilities, LA-UR-89-1021.